substance: Gd_2S_3
property: crystal structure, physical properties

α-Gd_2S_3

crystal structure	orthorhombic (D_{2h}^{16} – Pnma)			
lattice parameters				
a	7.339 Å		color: red	68P
b	15.273 Å			
c	3.932 Å			
a	7.338(2) Å			68S
b	15.273(3) Å			
c	3.932(2) Å			
electrical conductivity				
σ	25 Ω^{-1} cm^{-1}		(E_A = 0.007 eV)	68S
	$2 \cdot 10^{-3}$ Ω^{-1} cm^{-1}	n-type		70P
Seebeck coefficient				
S	– 360 μV K^{-1}		(referred to lead)	68S

Figures and further references for α-Gd_2S_3:

work function [67B]

absorption and luminescence spectra of Nd^{3+}-doped samples[80L], see also Figs. 1, 2

γ-Gd_2S_3

crystal structure	cubic (Th_3P_4-defect structure, T_d^6 –- $I\bar{4}3d$)			
lattice parameters				
a	8.387 Å			57F
	8.385 Å			81K
	8.3723(5) Å			73W
melting point				
T_m	1885ºC			57F
	1850ºC			81K
energy gap and other energy parameters				
E_g	3.4 eV	optical gap		82B
	1.4 eV		X-ray spectra	83S
E_b	5.8 eV	S 3p-level	MgKα XPS, Fig. 3 (E_b rel. to E_F)	91K
	9.5 eV	Gd 4f-level	MgKα XPS, Fig. 3	
	23.0 eV	Gd $5p_{3/2}$-level	MgKα XPS, Fig. 3	
	27.0 eV	Gd $5p_{1/2}$-level	MgKα XPS, Fig. 3	
	44.5 eV	Gd 5s-level	MgKα XPS, Fig. 3	
	143 eV	Gd $4d_{5/2}$-level	MgKα XPS, Fig. 4	
	149 eV	Gd $4d_{3/2}$-level	MgKα XPS, Fig. 4	
E_b	273 eV	Gd ($4p_{3/2}$, $4p_{5/2}$)-lev.	MgKα XPS	
	1188 eV	Gd $3d_{5/2}$-level	AlKα XPS, Fig. 5	
	1220 eV	Gd $3d_{3/2}$-level	AlKα XPS, Fig. 5	
E	8.2 eV	S 3p-E_F	ELS, Fig. 6	
	12.1 eV	S 3p-cond. band, surface plasmon	ELS, Fig. 6	91K
	17.3 eV	bulk plasmon	ELS, Fig. 6	
	24.9 eV	Gd 5p-E_F	ELS, Fig. 6	

	34 eV	Gd 5p-5d	ELS, Fig. 6	
	≈ 50 eV	Gd 5s-E_F	ELS, Fig. 6	
	149 eV	Gd 4d-4f	ELS, Fig. 7	

electrical conductivity

σ	250 Ω^{-1} cm^{-1}	n-type	74T
	10^{-8} Ω^{-1} cm^{-1}		82B

activation energy for conductivity

E_A	1.6...1.9 meV	77T

Further figures and references:

phase diagram: Fig. 8

coordination polyhedra: Fig. 9

thermal conductivity: Fig. 11

Raman and IR spectra: Fig. 10

temperature dependence of **resistivity, Hall coefficient, Seebeck coefficient**: Figs. 12...14

References:

57F Flahaut, J., Guittard, M., Loners, M. J., Patrie, M.: C. R. Acad. Sci. Paris 245 (1957) 2291.

66H Holtzberg, F., Methfessel, S.: J. Appl. Phys. 37 (1966) 1433.

67B Berkooz, O., Malamud, M., Shtrikman, S.: Solid State Commun. 6 (1967) 185.

68P Prewitt, C. T., Sleight, A. W.: Inorg. Chem. 6 (1968) 1090.

68S Sleight, A. W., Prewitt, C. T.: Inorg. Chem. 7 (1968) 2282.

70P Piekarzczyk, W., Peshev, P.: J. Crystal Growth 6 (1970) 357.

73W Wu, R., Gilles, P. W.: J. Chem. Phys. 59 (1973) 6136.

74T Taher, S. M. A., Gruber, J. B., Olsen, L. C.: J. Chem. Phys. 69 (1974) 2050.

77T Taher, M. A., Gruber, J. B.: Phys. Rev. B 16 (1977) 1624.

80L Leiss, M.: J. Phys. C 13 (1980) 151.

81K Kamarzin, A. A., Mironov, K. E., Sokolov, V. V., Malovitskii, Y. N., Vasil'yeva, I. G.: J. Cryst. Growth 52 (1981) 619.

82B Batirov, T. M., Verkhovskaya, K. A., Kamarzin, A. A., Malovitskii, Y. N., Lisoivan, V. I., Fridkin, V. M.: Sov. Phys. Solid State 24 (1982) 746.

83S Soldatov, A.V., Gusatinskii, A.N., Karin, M.G., Sidorin, K.K., Sadovskaya, O.A.: Inorg. Mater. 19 (1983) 951-954.

91K Kaciulis, S., Latisenka, A., Plesanovas A.: Surf. Sci. 251/252 (1991) 330.

Fig. 1.

α-Gd_2S_3:Nd, β-La_2S_3:Nd, Y_2S_3:Nd. Absorbance *A* vs. wavelength [80L].

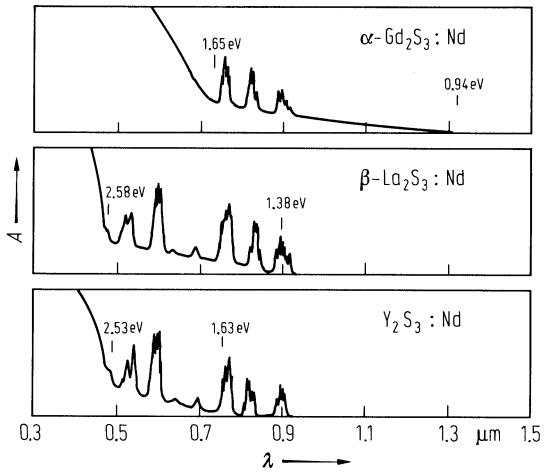

Fig. 2.

α-Gd_2S_3:Nd, β-La_2S_3:Nd, Y_2S_3:Nd. Photoluminescence intensity vs. wavelength for α-Gd_2S_3:Nd excited at 752.5 nm, β-La_2S_3:Nd and Y_2S_3:Nd excited at 600 nm [80L].

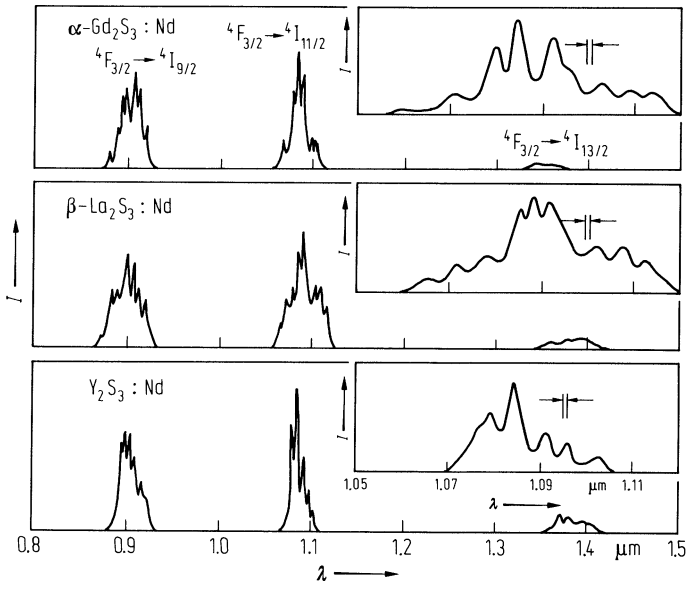

Fig. 3.

γ-Ln_2S_3. MgK_α X-ray photoelectron spectra of the rare-earth sesquisulfides (Ln = La, Ce, Nd, Sm, Gd, Dy) in the energy region below Fermi level down to Ln 5s core level [91K].

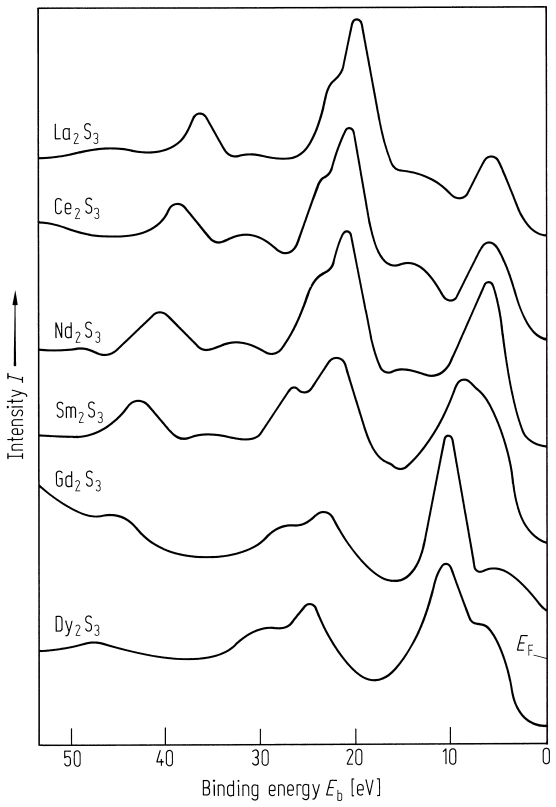

Fig. 4.

γ-Ln_2S_3. MgK_α X-ray photoelectron spectra of the rare-earth sesquisulfides (Ln = La, Ce, Nd, Sm, Gd, Dy) in the 4d core level region [91K]. E_b relative to E_F.

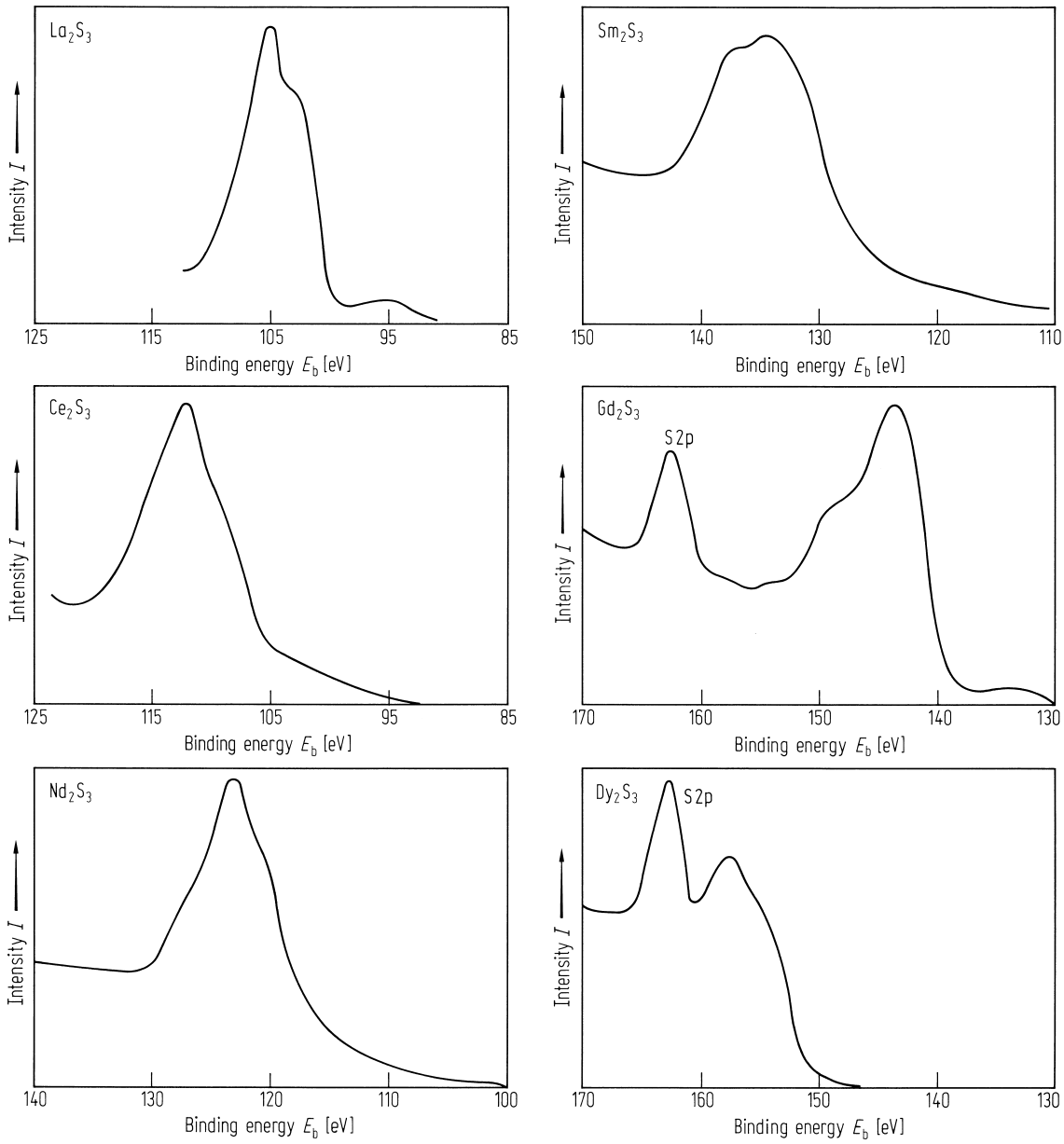

Fig. 5.

γ-Ln_2S_3. AlK_α X-ray photoelectron spectra of the rare-earth sesquisulfides (Ln = La, Nd, Sm, Gd) in the 3d core level region [91K]. The trivalence of Sm is testified by the value of the Sm 3d doublet line spin-orbit splitting (= 27.6 eV). E_b relative to E_F.

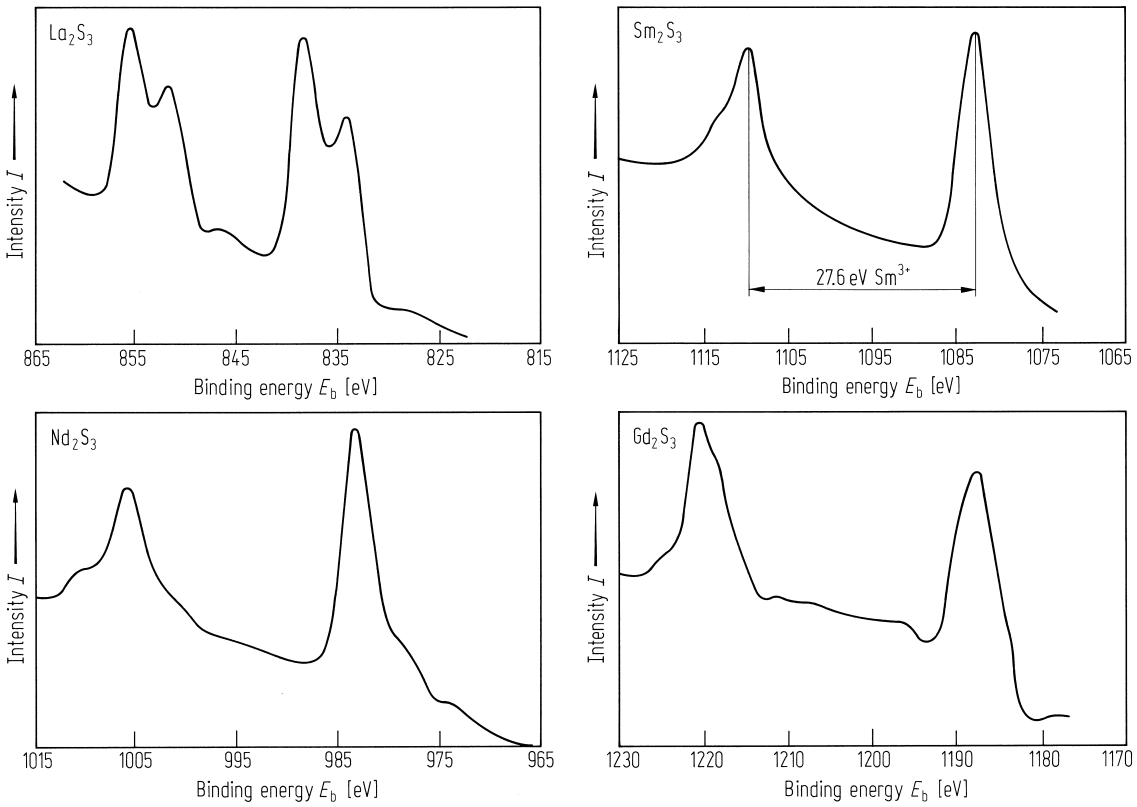

Fig. 6.

γ-Ln_2S_3. Electron loss spectra of the rare-earth sesquisulfides (Ln = La, Ce, Nd, Sm, Gd, Dy) for primary electron beam energy E_p = 750 eV. All the peaks, revealed from the second derivative d^2N/dE^2 are indicated by arrows [91K].

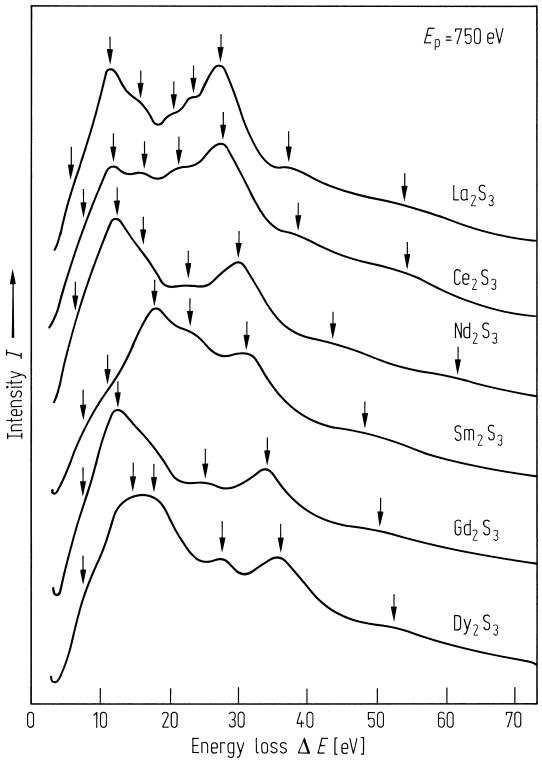

Fig. 7.

γ-Ln_2S_3, Ln = La, Nd, Gd. 4f-4f giant resonance in energy loss spectra at primary electron energy E_p = 750 eV after Shirley background subtraction [91K].

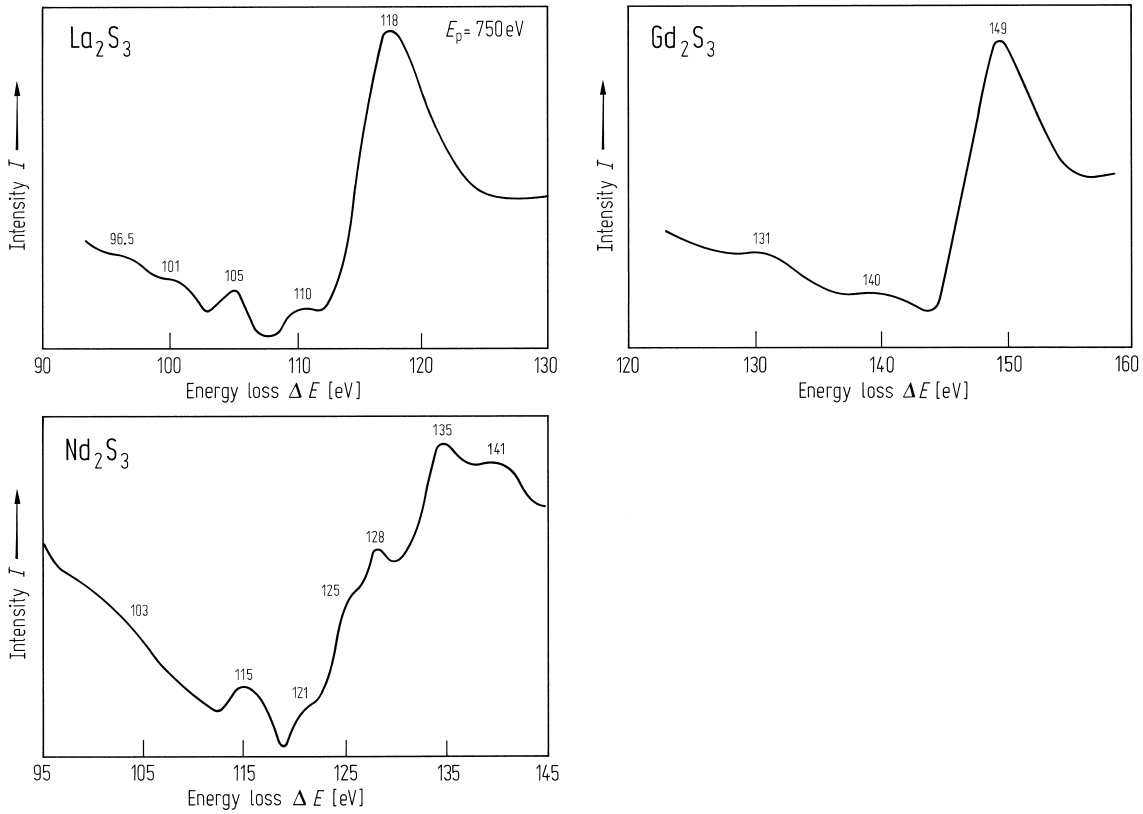

Fig. 8.

$LnS–Ln_2S_3$ system, Ln = La, Gd, Dy. Phase diagrams [81K].

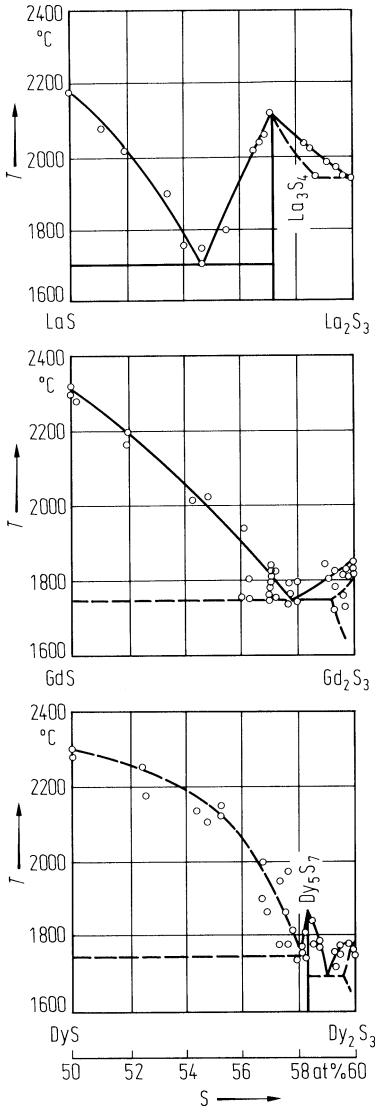

Fig. 9.

Th_3P_4-type compounds. The coordination polyhedra of the cations and the anions. Full circles: Th- atoms, other circles: P-atoms [66H].

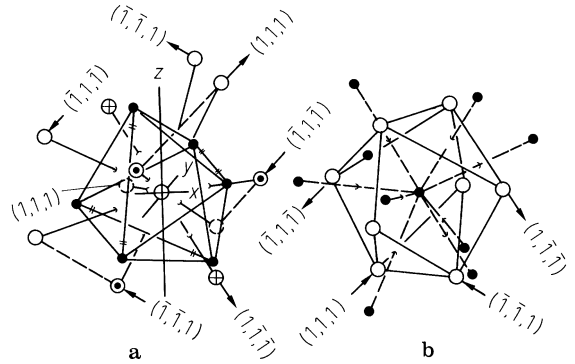

Fig. 10.

γ-La_2S_3, γ-Gd_2S_3. Infrared absorption and Raman intensity vs. wavenumber at 300 K [67B].

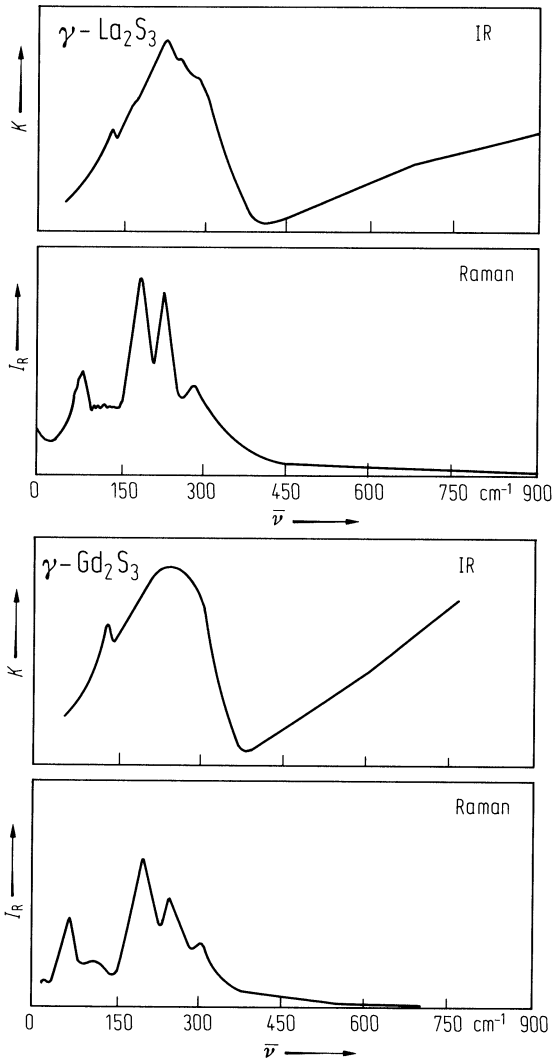

Fig. 11.

γ-Nd_2S_3, γ-Gd_2S_3, γ-Dy_2S_3. Thermal conductivity vs. temperature of several single crystals. The samples show the following excess metal content: Nd_2S_3 (*1*): 0.7% Nd, Nd_2S_3 (*2*): 0.6% Nd, Gd_2S_3 (*1*): 0.4% Gd, Gd_2S_3 (*2*): 0.5% Gd, Dy_2S_3 (*1*): 0.1% Dy, Dy_2S_3 (*2*): 0.2% Dy [77T].

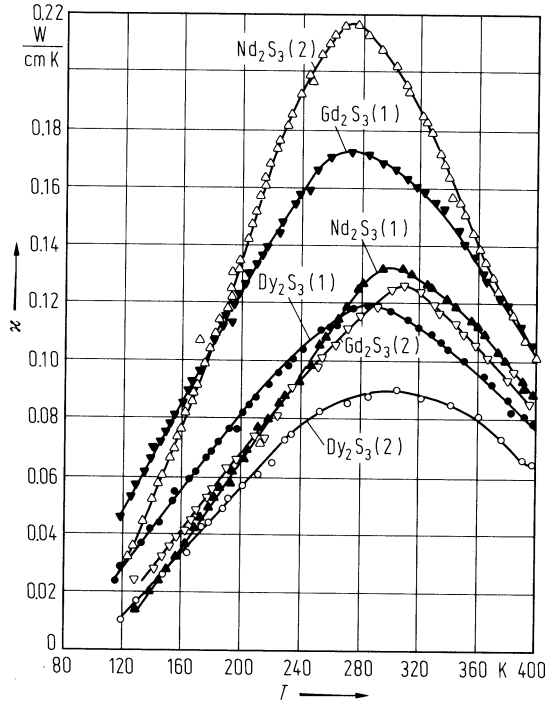

Fig. 12.

γ-Nd_2S_3, γ-Gd_2S_3, γ-Dy_2S_3. Temperature dependence of the electrical conductivity. The sample compositions are given in Fig. 11 [77T].

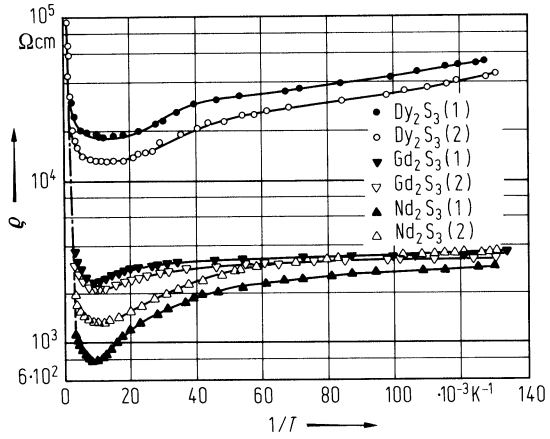

Fig. 13.

γ-Nd_2S_3, γ-Gd_2S_3, γ-Dy_2S_3. Thermoelectric power vs. temperature. The sample compositions are given in Fig. 11 [77T].

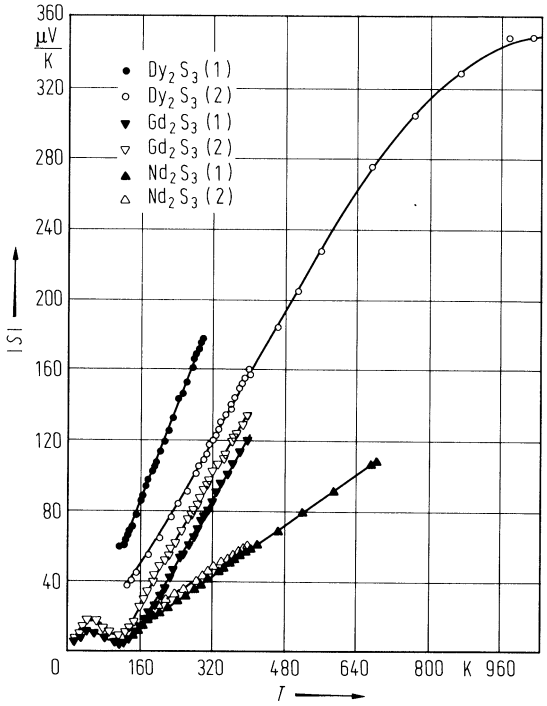

Fig. 14.

γ-Nd_2S_3, γ-Gd_2S_3. Absolute value of the Hall coefficient vs. temperature. The excess metal content is as follows: Nd_2S_3 (*1*): 0.7% Nd, Nd_2S_3 (*2*): 0.65% Nd, Gd_2S_3 (*1*): 0.6% Gd, Gd_2S_3 (*2*): 0.6% Gd [74T].